ORIGINAL RESEARCH

Surface engineered antifouling optomagnetic SPIONs for bimodal targeted imaging of pancreatic cancer cells

Xiaohui Wang[1]
Xiaohong Xing[1]
Bingbo Zhang[1]
Fengjun Liu[1]
Yingsheng Cheng[2]
Donglu Shi[1,3]

[1]Radiology Department of the Tenth People's Hospital, The Institute for Biomedical Engineering and Nano Science, Tongji University School of Medicine, Shanghai, People's Republic of China; [2]Department of Radiology, Shanghai Sixth People's Hospital, Shanghai Jiaotong University, Shanghai, People's Republic of China; [3]Materials Science and Engineering Program, Department of Mechanical and Materials Engineering, College of Engineering and Applied Science, University of Cincinnati, Cincinnati, OH, USA

Correspondence: Bingbo Zhang
Tongji University, Mailbox No 155,
1239 Siping Road, Shanghai, 200092,
People's Republic of China
Tel +86 21 65 983 706 819
Fax +86 21 65 983 7060
Email bingbozhang@tongji.edu.cn

Yingsheng Cheng
Shanghai Sixth People's Hospital,
Room 501, Teaching Building,
600 Yishan Road, Shanghai,
People's Republic of China
Tel +86 21 24 058 068
Fax +86 21 38 297 858
Email cjr.chengysh@vip.163.com

Abstract: Targeted imaging contrast agents for early pancreatic ductal adenocarcinoma diagnosis was developed using superparamagnetic iron oxide nanoparticles (SPIONs). For phase transfer of SPIONs, the hydrophobic SPIONs are first treated with tetrafluoroborate and then capped by bovine serum albumin (BSA) via ligand exchange. It was experimentally found that nitrosyl tetrafluoroborate pretreatment and proper structures of molecules are essential to the effective surface functionalization of SPIONs. Nonspecific binding was found to be significantly reduced by BSA surface functionalized hydrophobic SPIONs (BSA·SPIONs). The BSA·SPIONs were monodispersed with an average size of approximately 18.0 nm and stable in a wide pH range and various ionic strengths even after 7 days of storage. The longitudinal and transverse proton relaxation rate (r_1, r_2) values of the BSA·SPIONs were determined to be 11.6 and 154.2 s^{-1} per mM of Fe^{3+} respectively. The r_2/r_1 ratio of 13.3 ensured its application as the T_2-weighted magnetic resonance imaging contrast agents. When conjugated with near-infrared fluorescent dye and monoclonal antibody, the ^{dye}BSA·SPION-monoclonal antibody bioconjugates showed excellent targeting capability with minimal nonspecific binding in the bimodal imaging of pancreatic cancer cells. The experimental approach is facile, environmentally benign, and straightforward, which presents great promise in early cancer diagnosis.

Keywords: superparamagnetic iron oxide nanoparticles, BSA, bimodal imaging, MRI, targeted imaging

Introduction

Pancreatic ductal adenocarcinoma (PDAC), as a major disease with an extremely dismal 5-year survival rate below 5%, has attracted great attention not only in the medical communities but also in general public around the world.[1,2] Due to lack of accurate diagnostic tools, the majority of patients with advanced disease or metastasis exhibit considerable complications in surgery. Therefore, developing novel methods for early diagnosis is essential to improvement the PDAC survival rate.

Nano contrast agent (CA) based imaging with targeted functionalities show promise in early cancer diagnosis. Among the most commonly used nano CAs, superparamagnetic iron oxide nanoparticles (SPIONs) are of particular interest for their good biocompatibility, superior magnetic resonance (MR) T_2 (transverse relaxation) shortening effects, and biodegradability.[3–6] Furthermore, SPIONs exhibit large surface areas, making them favorable for versatile surface functionalization and conjugation of biomolecules.[7,8] Two most extensively used methods in preparing SPIONs for magnetic resonance imaging (MRI) are coprecipitation and thermal decomposition. The coprecipitation technique is probably the simplest chemical route in the preparation

of hydrophilic SPIONS. But this method does not provide good control on size distribution and particle geometry. In contrast, thermal decomposition in the oil phase can produce high quality hydrophobic iron oxide nanoparticles with perfect monodispersity and high crystallinity by modulating reaction temperature, reaction time, surfactant/precursor concentration, and type of solvent.[9] However, the obtained nanoparticles are usually hydrophobic and dispersible in organic solvent which requires further phase transfer procedures to make them water soluble. Various methods can be used for this phase transfer, such as polymer coating,[10] surfactant adsorption/exchange,[11] and silanization.[12] However, nonspecific binding is still a critical challenge for targeted diagnosis.[13,14] Nonspecific interaction of SPIONs with normal cell membranes may cause inefficient tagging to the desired targets, resulting in a high level of background signal that severely limits the contrast and sensitivity of the diagnostic imaging. Previous studies have shown that neutral and negatively charged SPIONs exhibit significant antifouling that can effectively reduce nonspecific binding.[15,16] Polyethylene glycol (PEG), known for its hydrophilic nature and biocompatibility, is often used to modify the surface properties of the nanoparticles for reduction of nonspecific binding and enhancement of colloidal stability and biocompatibility.[17,18] However, PEG surface functionalization decreases the volume fraction of magnetite, leading to reduced overall magnetic response of SPIONs.[19] The surface modification processes are also generally tedious, high cost, and environmentally unfriendly. It is, therefore, important to seek for other surface engineering routes with combined advantages in targeted imaging for early cancer diagnosis.

Bovine serum albumin (BSA) has been extensively used in biological applications due to its capability of reducing nonspecific binding in immunoassay,[20] commercial viability, and low cost. BSA is a zwitterionic surfactant with abundant carboxyl and amino groups. Such a unique structure not only provides sufficient binding sites for further functionalization, but also imparts good colloidal stability in both acidic and basic environments. In our previous work, we used BSA as the stabilizer and capping biopolymer, and successfully transferred hydrophobic quantum dots (QDs) and SPIONs into the hydrophilic phase under ultrasonication conditions.[21,22] The BSA coated QDs exhibited excellent antifouling property. The only difference found between the SPIONs and QDs was that the former clustered considerably while the latter individually dispersed in water solution. This is mainly attributed to the varied affinity of BSA from QDs to SPIONs.[21,22] The SPIONs formed clusters of nearly 100 nm and showed

appreciable MRI as a result of high uptake in liver. However, for the nonreticuloendothelial system, the nanoparticles must be kept small enough to escape the reticuloendothelial system for prolonged blood circulation time.[23]

Protein-based surface modification has been studied by a number of groups and shows advantages in biocompatibility, colloidal stability, high payload, and postmodifications.[24–26] As shown in Figure 1, a novel synthesis route is developed based on BSA surface engineering, aiming at procuring small (below 20 nm) and antifouling monodisperse magnetic nanoparticles with minimal nonspecific binding. Before BSA surface functionalization, the hydrophobic SPIONs are treated with tetrafluoroborate ($NOBF_4$). $NOBF_4$ treatment is a transition phase, having great advantages when compared to direct BSA surface functionalization of SPIONs in our previous work.[22] The purpose of this new approach is to exchange the organic ligands on SPIONs by $NOBF_4$. The $NOBF_4$-stabilized SPIONs are subsequently functionalized by BSA. This method is experimentally facile, effective, and reproducible. The as-prepared BSA surface functionalized hydrophobic SPIONs (BSA·SPIONs) exhibit good colloidal stability and high r_2 relaxivity. Upon conjugation with Cy5 dye (for near-infrared fluorescence [NIRF] imaging) and anti-plectin-1 monoclonal antibody (mAb), the resulting ^{dye}BSA·SPION-mAb bioconjugates demonstrate high specificity in recognition of plectin-1, a specific biomarker for PDAC,[27,28] in fluorescent and MR bimodal imaging.

Materials and methods
Materials
All reagents were purchased from Sigma-Aldrich (St Louis, MO, USA) and available commercially. Ultrapure Millipore deionized water (18.2 M$\Omega \cdot$cm resistivity at 25°C) was used throughout the experiments. Human PDAC cell lines Panc-1 and normal L02 cells were purchased from Cell Bank of the Chinese Academy of Sciences (Beijing, People's Republic of China) and cultured according to the established protocols.

BSA surface engineering of SPIONs
Hydrophobic SPIONs were synthesized according to a previously reported procedure.[9] BSA-stabilized SPIONs (BSA·SPIONs) were prepared by a two step process. The first step was $NOBF_4$ treatment on hydrophobic SPIONs aimed at exchanging the organic ligands of SPIONs. This procedure was performed according to a previously described method with slight modifications.[29] Briefly, 2 mL of SPIONs dispersion in n-heptane (approximately 5 mg/mL) was mixed with 10 mL of trichloromethane solution of $NOBF_4$ (0.01 M)
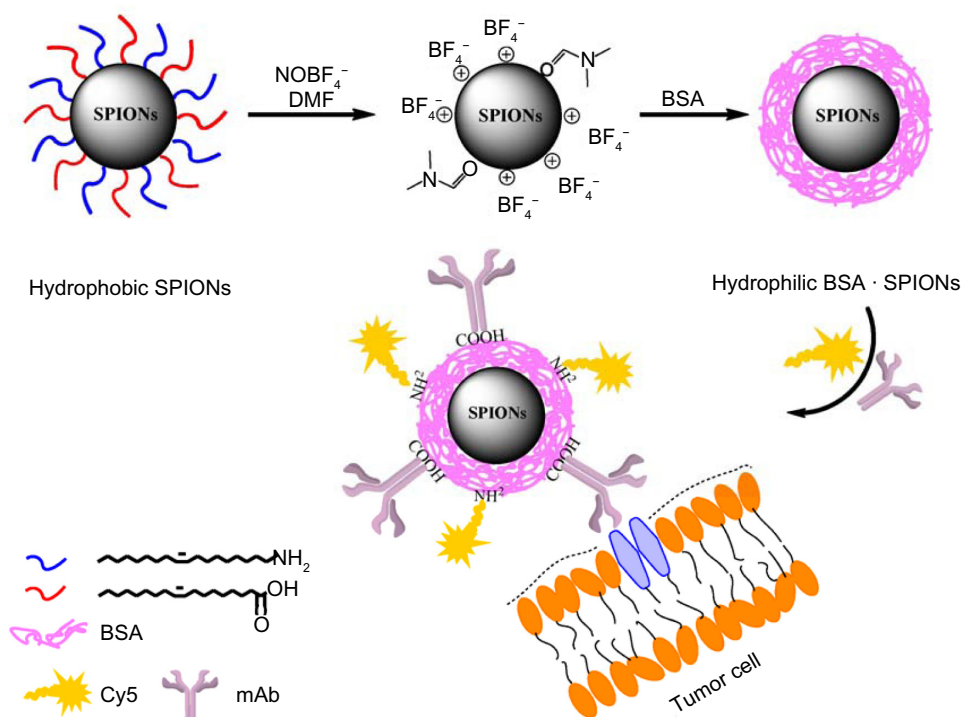
Figure 1 Schematic illustration of ^{dye}bovine serum albumin surface functionalized hydrophobic superparamagnetic iron oxide nanoparticles-monoclonal antibody bioconjugates.
Abbreviations: BSA, bovine serum albumin; BSA·SPIONs, bovine serum albumin surface functionalized hydrophobic superparamagnetic iron oxide nanoparticles; DMF, dimethylformamide; mAb, monoclonal antibody; NOBF$_4$, tetrafluoroborate; SPIONs, superparamagnetic iron oxide nanoparticles.

at room temperature. The resulting mixture was shaken gently until the precipitation of SPIONs was observed, typically within 5 minutes. After centrifugation to remove the supernatant, the precipitated SPIONs were redispersed in 2 mL of dimethylformamide (DMF) to form a stable colloidal dispersion. The second step was BSA surface functionalization. BSA (10 mg) was dissolved completely in 2 mL of deionized water and added into the above SPIONs/DMF solution followed by vigorous stirring for 2 hours at room temperature. The solution was then added into a dialysis bag (molecular weight cutoff of 8,000 Da to approximately 14,000 Da) and the dialysis bag was immersed in deionized water under shaking to displace DMF. The resulting aqueous solution was purified via ultracentrifugation twice (100,000× g, 30 minutes) to remove residual BSA. The final purified BSA·SPIONs were dispersed in borate saline buffer (50 mM, pH 8.2).

Preparation of ^{dye}BSA·SPION conjugates and ^{dye}BSA·SPION-mAb bioconjugates

The nontargeted ^{dye}BSA·SPION NIRF/MR bimodal imaging CAs were prepared by Cy5-mono N-hydroxysuccinimide ester directly reacting with the amino group on the BSA·SPIONs overnight in borate saline buffer (50 mM, pH 8.2) at room temperature. The excess Cy5 dye was removed by dialysis with a dialysis bag (molecular weight cutoff 8,000 Da to approximately 14,000 Da) against borate saline buffer (50 mM, pH 8.2). The conjugation of Cy5 dye to the BSA·SPIONs was determined by fluorescence spectroscopy.

The targeted ^{dye}BSA·SPION-mAb bioconjugates were prepared by a carbodiimide reaction linking anti-Plec-1 antibodies to the purified ^{dye}BSA·SPION conjugates using ethyl-3-(3-dimethylaminopropyl)carbodiimide hydrochloride (EDC·HCl) as the crosslinker. The ^{dye}BSA·SPIONs were reacted with monoclonal antibody at an appropriate Fe^{3+}/mAb/EDC·HCl molar ratio in borate saline buffer (50 mM, pH 8.2) for 2 hours at room temperature. The final bioconjugates were dispersed in phosphate buffered saline ([PBS] 0.01 M, pH 7.4, 0.5% BSA, 0.02% sodium azide) after being purified by ultracentrifugation at 100,000× g for 15 minutes and washed with 0.01 M PBS (pH 7.4) twice. The conjugation of anti-Plec-1 antibodies was confirmed using a test trip on the basis of the primary and secondary antibody response.[30]

Material characterization and statistical analysis

Transmission electron microscopy (TEM) was carried out on a JEOL JEM-1230 TEM (JEOL, Tokyo, Japan) with a tungsten

filament at an accelerating voltage of 200 kV. The sample was prepared by placing a drop of prepared sample on the surface of copper grids and dried at room temperature. Fourier transform infrared spectra (FTIR) were obtained on a TENSOR 27 FTIR spectrometer (Bruker Corporation, Billerica, MA, USA) over a potassium bromide pellet. The samples dispersed in different solutions (chloroform for SPIONs, DMF for NOBF4·SPIONs, water for BSA and BSA·SPIONs) were dried before FTIR analysis. The crystalline structures of the as-prepared samples were evaluated by X-ray diffraction (XRD) analysis on a DX-1000 diffractometer (Dandong Fangyuan Instrument Co., Ltd., Dandong, People's Republic of China) by using CuK_α radiation (λ=0.15406 nm). The operation tube voltage and current were kept at 40 kV and 30 mA, respectively. Dynamic light scattering (DLS) data of the samples in borate buffer was taken using a particle size analyzer (Nano ZS90; Malvern Instruments, Malvern, UK). Laser scanning confocal images were collected on a laser scanning confocal microscope (Leica TCS SPS; Leica Microsystems, Wetzler, Germany). Emission spectra were observed on a LS-55 spectrophotometer (Perkin Elmer, Waltham, MA, USA). The magnetic characterization was carried out with a vibrating sample magnetometer on a LDJ9600-1 physical property measurement system (LDJ Electronics, Troy, MI, USA) at 300 K. Statistical analysis was performed using SPSS18.0 (SSPS Inc., Chicago, IL, USA).

Colloidal stability study of BSA·SPIONs

The prepared BSA·SPIONs were dissolved in various pH buffer solutions (pH value varied from 4 to 13) and sodium chloride water solutions (ionic strength varied from 0.01 M to 1 M) for 7 days at room temperature. The DLS analyses were performed to evaluate the hydrodynamic diameters and zeta potentials of the samples in every solution.

In vitro relaxometry

The longitudinal and transverse relaxation times were determined using a 1.41 T minispec mq 60 NMR Analyzer (Bruker Optik GmbH, Ettlingen, Germany) at 37°C. The relaxivity values of r_1 and r_2 were calculated by fitting the $1/T_1$ and $1/T_2$ relaxation time (s^{-1}) versus Fe^{3+} concentration (mM) curves. The in vitro MR images of BSA·SPIONs were obtained using a head coil of Siemens MRI system (MAGNETOM Verio; Siemens Healthcare, Munich, Germany). The measurement conditions were as follows: T_2-weighted sequence, multislice spin echo, repitition time/echo time (TR/TE)=4,800/80 ms, matrix acquisition=134×192, number of excitations (NEX)=3, field of view (FOV)=63 mm×63 mm, FOV phase of 100%, thickness=2.5 mm, 3 T, 25°C.

In vitro laser scanning confocal imaging and MRI

Panc-1 cell lines (Plec-1 overexpressed)[27] were used in this study to evaluate the specificity of the [dye]BSA·SPION-mAb bioconjugates. Cells were cultured in Dulbecco's Modified Eagle's Medium (high glucose) mixture with 10% fetal bovine serum and penicillin/streptomycin (100 U/mL) at 37°C in a humidified atmosphere containing 5% CO_2. Cells were plated in glass-bottomed microwell dishes and cultured for 24 hours. Following this, 2 mM (Fe^{3+}) of Plec-1-targeted [dye]BSA·SPION-mAb bioconjugates and nontargeted [dye]BSA·SPION conjugates was added into the Panc-1 cells, respectively, and incubated with the corresponding cells for 5 minutes. After being washed twice with 0.01 M PBS, the cells were imaged under a laser scanning confocal microscope (Leica TCS SPS; Leica Microsystems).

For in vitro cell MRI experiments, the cells were incubated with Plec-1-targeted [dye]BSA·SPION-mAb bioconjugates and nontargeted [dye]BSA·SPION conjugates, respectively, at 37°C for 2 hours. Cells were washed and then redispersed in eppendorf tubes. The tubes were scanned in a 3 T MRI scanner (MAGNETOM Verio; Siemens Healthcare) using multiecho T_2 weighted fast-spin echo imaging sequences (head coil, TR/TE =4,800/80 ms, matrix acquisition =128 × 128, NEX =3, FOV =60 × 60 mm, FOV phase of 100%, thickness =2 mm, 3 T, 25°C).

To evaluate the targeting capability of [dye]BSA·SPION-mAb bioconjugates, a competitive inhibition cell assay was performed in both fluorescent and MR imaging by adding free Plec-1 monoclonal antibodies (10 µL, 0.1 mg/mL) into Panc-1 cells for preincubation before introduction of the Plec-1-targeted [dye]BSA·SPION-mAb bioconjugates.

Cytotoxicity assay

In vitro cytotoxicity was assessed on L02 cells, using a modified 3-(4, 5-dimethylthiazol-2-yl)-2, 5-diphenyl-tetrazolium bromide (MTT) method.[31] Before application of the surface saturated SPIONs to the MTT assays, some necessary steps were performed including introduction of the nanoparticles into the cell medium and leaving the solution in contact for a period of 24 hours, and then replacing with a fresh medium. Cells (100 µL) growing in the log phase were seeded in a 96-well flat culture plate at $1 × 10^4$ cells per well and subsequently incubated for 24 hours at 37°C under 5% CO_2. The pretreated BSA·SPIONs samples with different concentrations were added to each group (six wells) for 24 hours. MTT solution (10 µL, 5 mg/mL in PBS) was added to the wells and

incubated for an additional 4 hours. MTT internalization was terminated by aspiration of the media, and the cells were lysed with dimethylsulfoxide (150 μL/well). The absorbance of the suspension was measured at 570 nm (intensity of absorbance [IA] value) on a Tecan Infinite M200 monochromator-based multifunction microplate reader (Tecan Group Ltd, Mannedorf, Switzerland) with background subtraction at 690 nm. The following formula was used to calculate the viability of cell growth: cell viability (%) = (mean of IA value of treatment group/mean of IA value of control) ×100.

Results and discussion
Phase transfer of SPIONs

BSA is a water soluble macromolecule containing one single cysteine and eight pairs of disulfide bonds.[32] These sulfhydryl compounds can act as multidentate ligands that replace the original ones on some hydrophobic nanoparticles via ligand exchange.[33–35] Based on the unique structure of BSA, it was found that the QDs were effectively surface functionalized under ultrasonication.[21] However, SPIONs were found to cluster at an average size of 100 nm.[22] In this study, a transition process by $NOBF_4$ was introduced to the surface functionalization of SPIONs.

Figure 1 illustrates the synthesis route of $^{dye}BSA·SPION$-mAb bioconjugates. BSA·SPIONs are designed as the nano carrying systems for construction of the $^{dye}BSA·SPION$ and $^{dye}BSA·SPION$-mAb conjugates. The originally synthesized SPIONs are hydrophobic and only soluble in nonpolar solvents such as n-heptane due to their surface organic ligands. As shown in Figure 1, the first treatment involves adding $NOBF_4/DMF$ to the SPION/n-heptane solution. After gentle shaking of the mixture solution, flocculation is observed, indicating solubility change of SPIONs as a result of $NOBF_4$ surface modification. After slight centrifugation to remove the supernatant, the precipitated SPIONs can be readily redispersed in various hydrophilic solvents such as DMF without precipitation.

The hydrophilic nature suggests the removal of the original organic ligands, which was further verified by FTIR analysis (Figure S1). The FTIR spectra of SPIONs show the intensity of the characteristic C–H stretching vibrations around 2,800 cm^{-1} ascribed to oleic acid molecules. A new peak at 1,028 cm^{-1} in the $NOBF_4·SPIONs$ spectrum, which is assigned to BF_4^- anions,[36] suggests an exchange between the organic ligands and inorganic BF_4^- anions. Another peak around 1,630 cm^{-1} can be attributed to C=O stretching vibrations of the solvent DMF molecules.[29] The remaining broad band around 3,500 cm^{-1} is attributable to the solvated

water molecules, accordant with the hydrophilic nature of the SPIONs dispersion.

It is worth noting that dispersing $NOBF_4·SPIONs$ in water results in partial aggregations, even though $NOBF_4·SPIONs$ have high solubility in DMF, a polar (hydrophilic) aprotic solvent miscible with water and majority of organic liquids. It indicates the poor compatibility of $NOBF_4·SPIONs$ with water molecules, an issue that has to be addressed for biological applications. Hydrophilic BSA protein was selected for further surface treatment of $NOBF_4·SPIONs$. This step was important for stabilizing SPIONs in water without precipitation and reducing nonspecific cellular binding.

Upon BSA surface functionalization, SPIONs were found to disperse well in water without aggregation. The dispersion is associated with the successful coating of BSA via secondary ligand exchanging (Figure 1). FTIR analysis provides the evidence of BSA on the SPIONs surfaces (Figure S1). The BSA·SPIONs exhibit two additional bands at 1,350 cm^{-1} and 1,650 cm^{-1} which are identical to those on pure BSA. The reduced peak at 1,028 cm^{-1} indicates the removal of BF_4^- anions on the surface of SPIONs. In BSA surface functionalization, removal of DMF is found to be necessary for the formation of stable BSA·SPIONs in water solution. As shown in Figure S2, the BSA·SPIONs dialyzed against deionized water can be well dispersed in deionized water and the dispersion is optically clear without obvious aggregates or sediments after 7 days of storage. On the contrary, without dialysis to remove DMF, the as-synthesized nanoparticles sink rapidly in deionized water. These results suggest that DMF can inhibit BSA interaction with $NOBF_4·SPIONs$. $NOBF_4·SPIONs$, having a high solubility in DMF, are inclined to huddle with DMF molecules even though BSA is present in the DMF/water solution.[29] However, in the course of dialysis against water, the inhibition of DMF decreases along with DMF being diluted gradually in the samples. Therefore, hydrophilic BSA can be anchored onto the surfaces of SPIONs by means of its chemical groups with appreciable metal affinity,[21] resulting in enhanced solubility of BSA·SPIONs in water.

Other water soluble compounds such as dopamine hydrochloride and PEG derivatives were used to stabilize SPIONs after the $NOBF_4$ treatment using the same approach. However, these treatments result in serious SPIONs sediments in deionized water (Figure S3). It indicates that the molecular structures of these compounds play important roles in the surface functionalization of SPIONs. Compared with the low molecule compounds, the multiple anchoring

sites on the BSA macromolecule enable high affinity with the surface metal atoms of SPIONs and therefore enhance the colloidal stability of BSA·SPIONs.[21] The abundant amino/carboxyl groups of BSA are favorable to post surface modifications with other functional materials such as antibody and fluorescent dye.

The BSA·SPIONs synthesized by this approach are monodisperse and uniform. The shape of the nanoparticles is maintained after surface modification (Figure 1A and B). No aggregation is observed, which is further confirmed by the DLS analysis (Figure 1C). As shown in the DLS data, the size of BSA·SPIONs is slightly larger than that observed from TEM. This is attributed to macromolecules being capped on SPIONs. The diameter of the as-synthesized hydrophobic SPIONs is about 8.0 nm, and the BSA macromolecule in water is about 5.0 nm in size.[37] Accordingly, the diameter of BSA·SPIONs is about 18.0 nm $(8.0 + 2 \times 5.0)$, coinciding with the hydrodynamic diameter analyzed by DLS.

The as-prepared BSA·SPIONs have excellent water solubility and colloidal stability (Figure 2). Figure 2A shows the colloidal stability of the BSA·SPIONs at various pH values. Over a wide range of pH values (pH 4–13), the BSA·SPIONs solutions are optically clear without aggregations, except for the sample at pH 5.6. This is due to BSA·SPIONs being close to electroneutrality at pH 5.6, leading to a large number of precipitations (Figure 3C). BSA·SPIONs also exhibit good stability in sodium chloride water solutions with various ionic strengths (from 0.01 M to 1 M, Figure 2B).

The phase transformation of SPIONs from organically soluble to water soluble was successfully achieved in this study. Instead of chloroform, the as-prepared BSA·SPIONs can only be solubilized in aqueous solution (Figure 2C). The DLS data on the hydrodynamic diameters of BSA·SPIONs at diverse pH values and ionic strengths (Figure 3) also show its excellent colloidal stability.

As is well known, BSA is rich in the amino and carboxyl groups which can offer an effective cushioning effect in both acidic and alkaline solutions. Therefore, BSA surface functionalization enables the nanoparticles to be ionized at various pH values and resistant to harsh chemical surroundings. These experimental results (pH approximately 7.4 and high ionic concentration) show favorable surface properties of BSA·SPIONs for intracellular and in vivo studies.

In vitro relaxivity characterization of BSA·SPIONs

SPIONs were synthesized for MRI for their known superparamagnetism. As can be seen in Figure 4A, all XRD diffraction peaks can be indexed to typical pattern of Fe_3O_4 (Joint Committee on Powder Diffraction Standards [JCPDS] 75-1609). Figure 4B shows the hysteresis loops of SPIONs at room temperature. The reversible hysteresis curves indicate the superparamagnetic nature of the nanoparticles.

The longitudinal (T_1) and transverse proton relaxation times (T_2) of BSA·SPION water solutions at different concentrations were measured as a function of Fe^{3+} concentration at 1.41 T, 37°C. As shown in Figure 5A, the r_2 value of the BSA·SPIONs was as high as 154.2 s^{-1} per mM of Fe^{3+}. The r_2/r_1 value of 13.3 indicates significant advantage of BSA·SPIONs as negative MRI CAs. Only low dosage CA may be needed for imaging at high relaxivity. This is particularly useful for patients with weak organ functions.[38] The T_2-weighted MR images of BSA·SPIONs at various concentrations in Figure 5B give further evidence for favorable MRI application. MR signal intensities of the BSA·SPIONs water solutions are progressively reduced with decreasing Fe^{3+} concentration.

It is well known that the surface of nanoparticles is capped by biomolecules (proteins, sugars, and lipids) upon coming into contact with biological systems, resulting in the formation of a protein "corona" that is strongly associated with the nanoparticle surface.[39] Therefore, the MR relaxivity of nanoparticles could be affected by this protein "corona".[40] In this study,
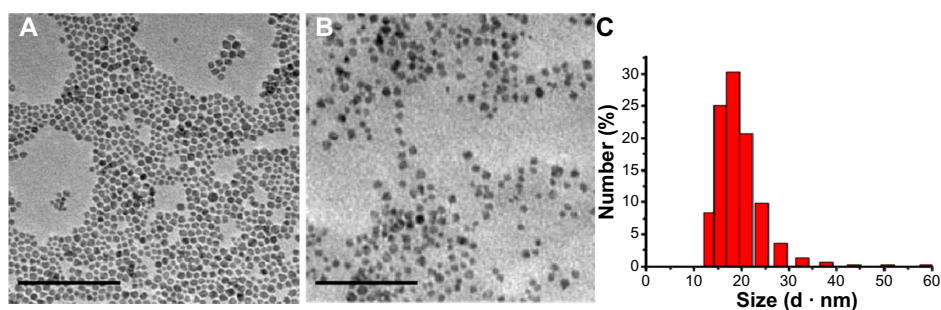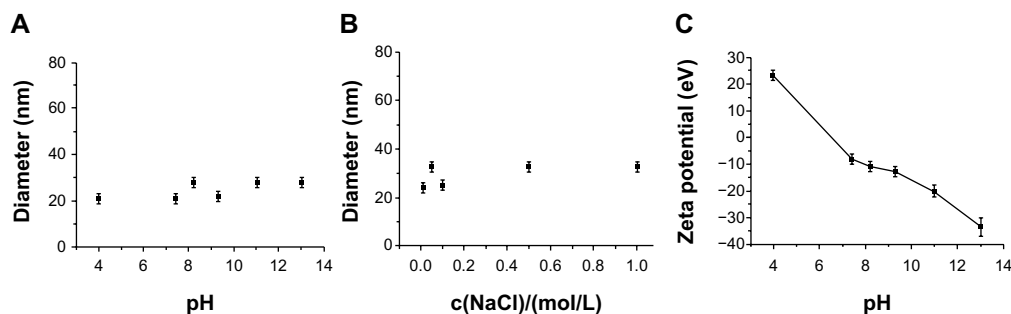

Figure 1 Transmission electron microscopy images of hydrophobic superparamagnetic iron oxide nanoparticles.
Notes: (**A**) Superparamagnetic iron oxide nanoparticles (SPIONs) in chloroform and (**B**) bovine serum albumin surface functionalized hydrophobic SPIONs (BSA·SPIONs) in borate buffer without size selection. (**C**) Dynamic light scattering data of the BSA·SPIONs in borate buffer. Scale bar is 100 nm.
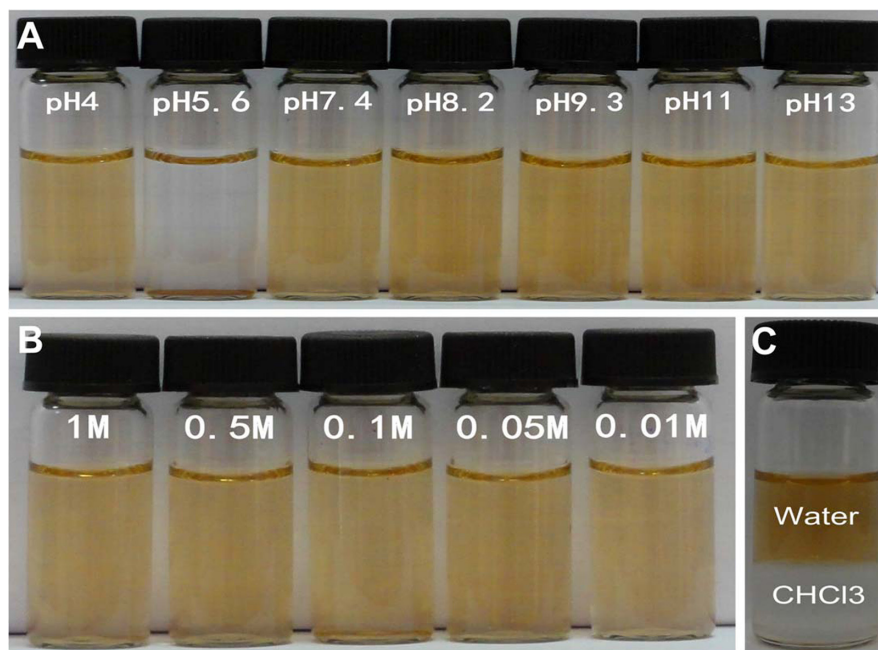
Figure 2 Digital images of the bovine serum albumin surface functionalized hydrophobic superparamagnetic iron oxide nanoparticles in corresponding solutions with different pH values.
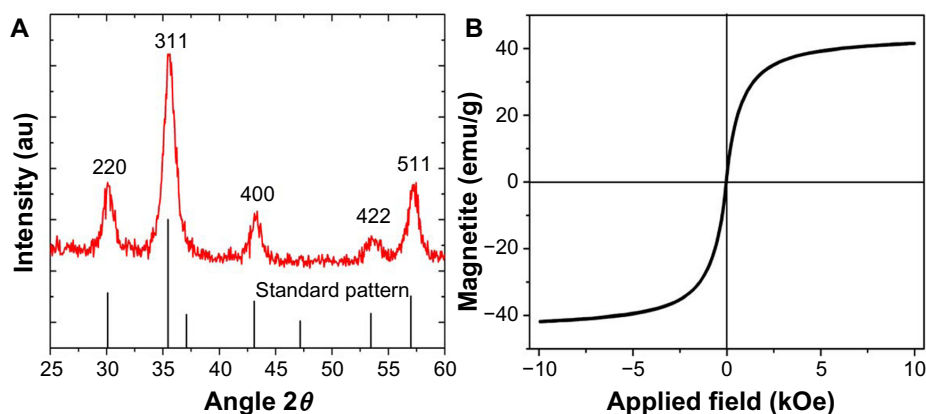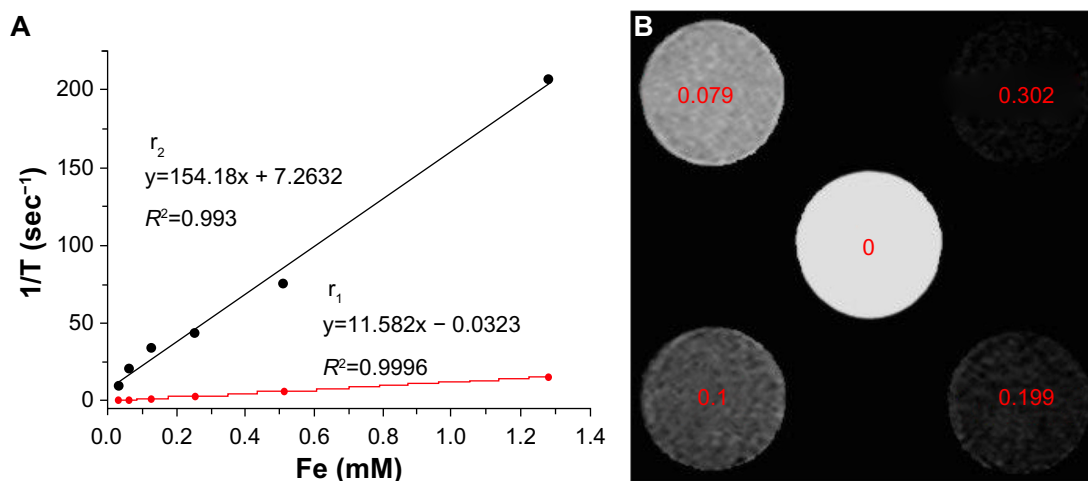**Notes:** (**A**) Bovine serum albumin surface functionalized hydrophobic superparamagnetic iron oxide nanoparticles (BSA·SPIONs) corresponding solutions with different pH values and (**B**) with various ionic strengths in sodium chloride water solutions with (**C**) demonstration of successful phase transfer of the BSA·SPIONs. All samples before optical photography were placed at room temperature for 7 days of storage.

Figure 3 The hydrodynamic diameters of the bovine serum albumin surface functionalized hydrophobic superparamagnetic iron oxide nanoparticles.
Notes: (**A**) Bovine serum albumin surface functionalized hydrophobic superparamagnetic iron oxide nanoparticles (BSA·SPIONs) at various pH buffer solutions and (**B**) in sodium chloride water solutions with different ionic strengths analyzed by dynamic light scattering after 7 days of storage at room temperature. (**C**) The zeta potentials of BSA·SPIONs at various pH buffer solutions.
**Abbreviation:** NaCl, sodium chloride.

Figure 4 Analysis of superparamagnetic iron oxide nanoparticles.
Notes: X-ray diffraction pattern (**A**) and magnetic hysteresis curve (**B**) of the hydrophobic superparamagnetic iron oxide nanoparticles.

Figure 5 Relaxivity curves and magnetic resonance images of BSA·SPIONs.
Notes: (**A**) The r_1 and r_2 relaxivity curves obtained from water solutions of bovine serum albumin surface functionalized hydrophobic superparamagnetic iron oxide nanoparticles (BSA·SPIONs). (**B**) T_2-weighted magnetic resonance images of BSA·SPIONs with various concentrations (from 0.079 to 0.302 mM Fe^{3+}).
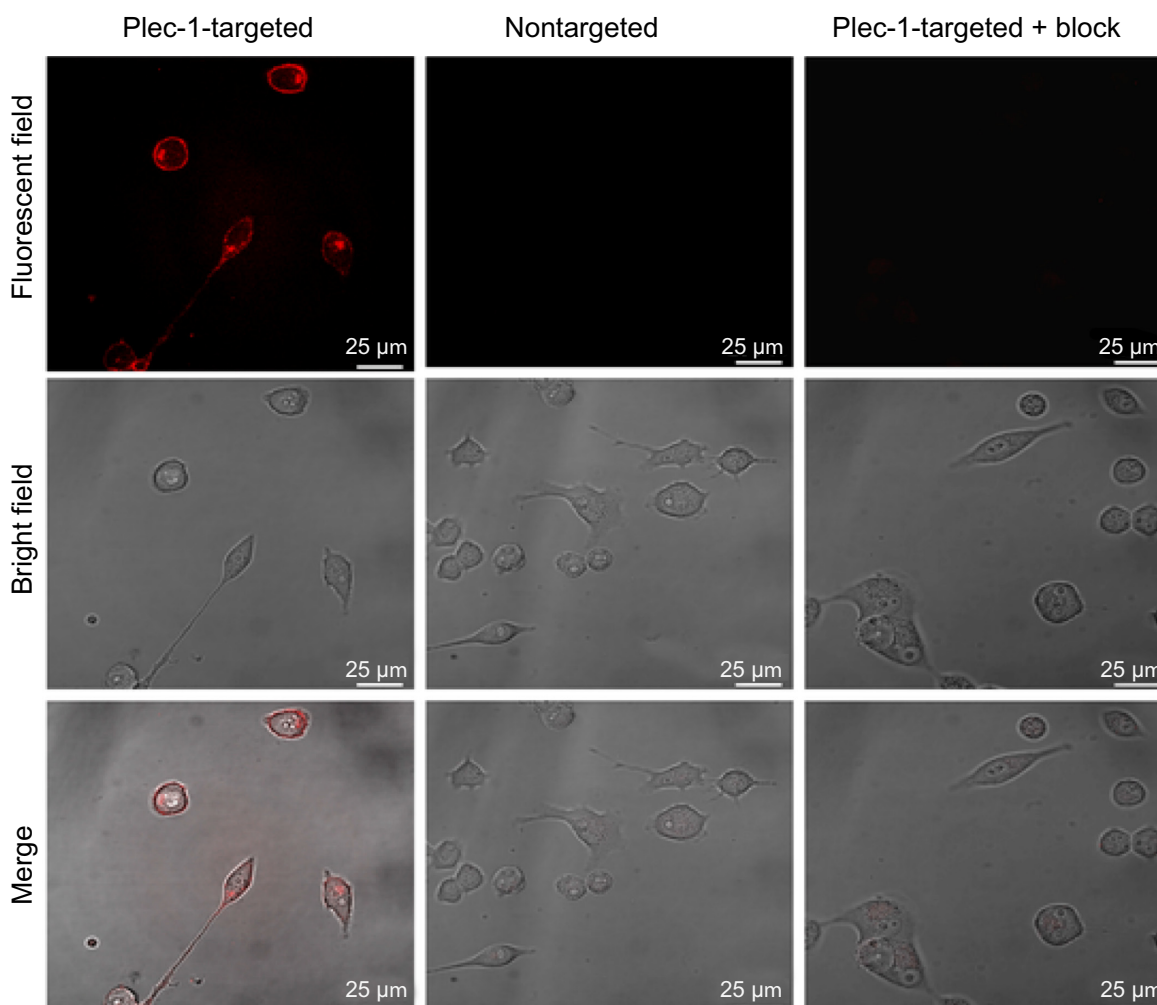
Figure 6 Targeted imaging of Panc-1 cells with Plec-1-targeted ^{dye}BSA·SPIONs-mAb bioconjugates.
Notes: Panc-1 cells (Plec-1-positive) were incubated with Plec-1-targeted and nontargeted bovine serum albumin surface functionalized hydrophobic superparamagnetic iron oxide nanoparticles (BSA·SPIONs) for 5 minutes. To further determine targeting specificity, cells were preincubated with free Plec-1 antibodies before adding Plec-1-targeted ^{dye}BSA·SPIONs-mAb bioconjugates.

BSA·SPIONs are precoated with BSA protein, which have antifouling properties and repressing the "corona" capability in a biological environment. It was found that BSA·SPIONs are suitable for MRI applications based on their relaxivity data.

In vitro laser scanning confocal and MR imaging

Successful conjugation of Cy5 dyes and anti-Plec-1 antibodies to BSA·SPIONs are demonstrated (Figure S4A) for targeted optical and MR imaging. As shown in the fluorescent spectra of the purified [dye]BSA·SPIONs conjugates, a clear peak is observed at 658 nm with 630 nm excitation. This is consistent with the fluorescent spectra of the free Cy5 dye, indicating that

the Cy5 dyes are successfully conjugated to the BSA·SPIONs nanoparticles. To verify the conjugation of anti-Plec-1 antibodies to [dye]BSA·SPIONs, a test strip technology was used for the secondary antibodies to recognize the primary antibodies on nanoparticles.[30] As can be seen in Figure S4B, there is a distinguishable narrow and yellow band on the test strip for the [dye]BSA·SPIONs-mAb bioconjugate, but no signal is observed for the nontargeted [dye]BSA·SPIONs conjugate. It is concluded, therefore, the anti-Plec-1 primary antibodies were successfully conjugated to the [dye]BSA·SPIONs nanoparticles. The absence of [dye]BSA·SPIONs at the site of secondary antibodies line shows their potent antifouling capability, which is favorable for the following cell targeted imaging.
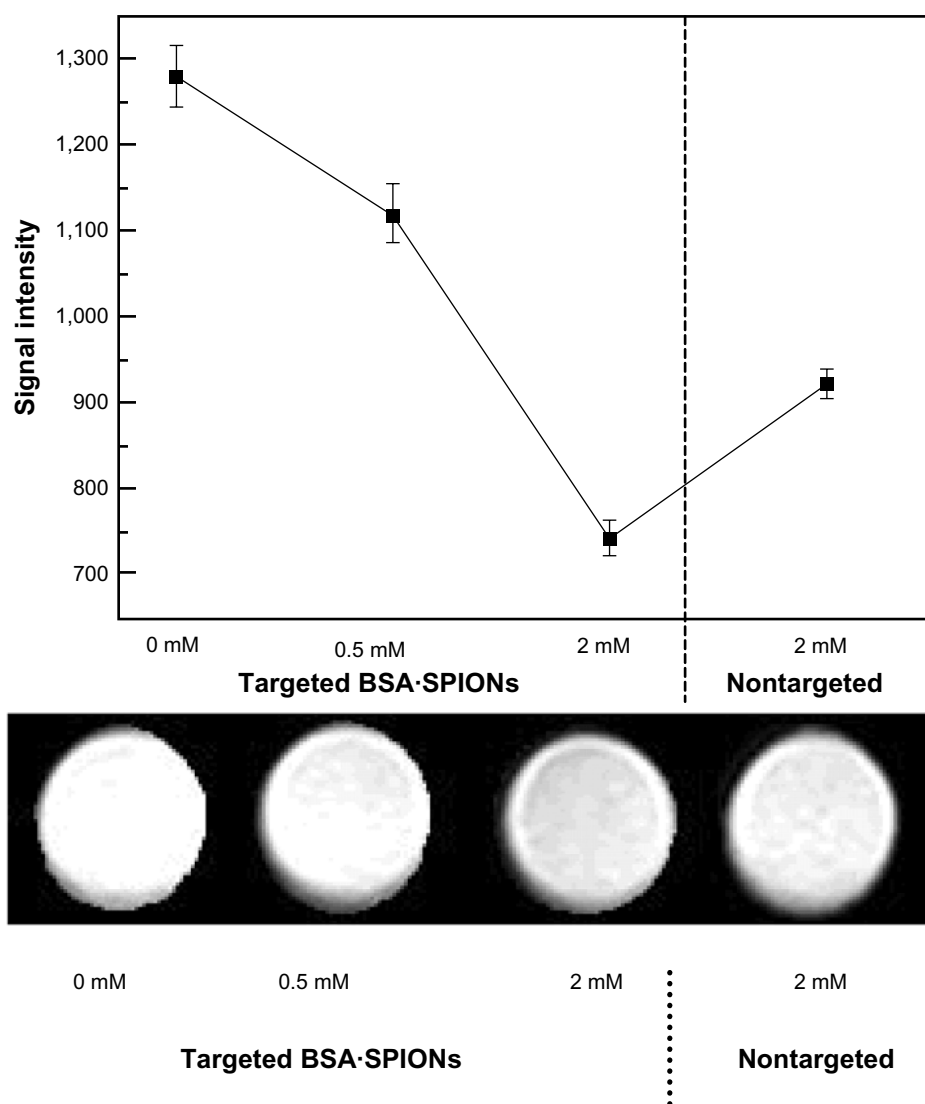
Figure 7 Magnetic resonance images of Panc-1 cells.
Notes: Signal intensity curve (top) and T_2-weighted (bottom) magnetic resonance imaging of Panc-1 cells incubated with Plec-1-targeted [dye]bovine serum albumin surface functionalized hydrophobic superparamagnetic iron oxide nanoparticles-monoclonal antibody bioconjugates (0 to 2 mM) and nontargeted [dye]bovine serum albumin surface functionalized hydrophobic superparamagnetic iron oxide nanoparticles conjugates (2 mM) for 2 hours.
Abbreviation: BSA·SPIONs, bovine serum albumin surface functionalized hydrophobic superparamagnetic iron oxide nanoparticles.

Figure 6 shows the targeting capability of Plec-1-targeted dyeBSA·SPIONs-mAb bioconjugates to Panc-1 cells (Plec-1 overexpressed).[27] The laser scanning confocal images show significant binding of Plec-1-targeted dyeBSA·SPIONs-mAb to the Panc-1 cells but not the nontargeted dyeBSA·SPIONs. This targeting specificity is further confirmed by competitive inhibition of the fluorescence cell assay. After blocking with free anti-Plec-1 antibodies, the binding of dyeBSA·SPIONs-mAb to the Panc-1 cells (Figure 6C) is significantly inhibited.

Nonspecific cellular binding of nanoparticles has been a complex issue. It is associated with hydrophobic interactions between the ligands of nanoparticles and lipids on the cell membranes. It can also be attributed to the electrostatic interactions between the cells and the charged nanoparticle surface functional groups.[13,16,17] BSA has been widely used for nonspecific binding reduction in biological detection.[21,41,42] In this study, the BSA surface tailored SPIONs was shown to exhibit superior antifouling on reduction of nonspecific cellular binding based on the cell assay results (Figure 6). BSA has been found in this study to serve two major functionalities, namely the ligand exchange for water solubilization of SPIONs and antifouling for reduction of nonspecific cellular binding.

The BSA protein surface engineered SPIONs can repress protein corona upon contact in the biological system. It is reported that protein corona can significantly reduce active targeting yield, because protein corona induced screening of nanoparticle targeting ligands.[43,44] In this study, BSA protein capped on SPIONs has the capability to reduce protein corona. Thus, the antibodies linked on the BSA are fully exposed to their targets on a separate surface. Also, cellular immunofluorescence assays have shown that they are targeting and are effective.

Panc-1 cell MR scanning was performed after incubation with Plec-1-targeted dyeBSA·SPIONs-mAb and nontargeted dyeBSA·SPIONs conjugates, respectively. As shown in Figure 7, Panc-1 cells incubated with Plec-1-targeted dyeBSA·SPIONs-mAb exhibit significant T_2 reduction when compared with nontargeted dyeBSA·SPIONs at the same concentration. The incubation time for MR scanning is 2 hours, which is much longer than that for fluorescent imaging (5 minutes). The samples after 5 minutes of incubation show no signal changes in the MRI images due to its lower sensitivity compared to optical imaging. By extending incubation time, cellular internalization of nanoparticles results in nonspecific signal enhancement for nontargeted dyeBSA·SPIONs conjugates in both MR and fluorescent imaging (Figure S5). It is worth noting that the Plec-1-targeted dyeBSA·SPIONs-mAb bioconjugates are mainly located on the cell membrane with few nanoparticles internalized into cytoplasm, while the nontargeted dyeBSA·SPIONs predominately internalized into the cytoplasm of Panc-1 cells (Figure S5). This difference is
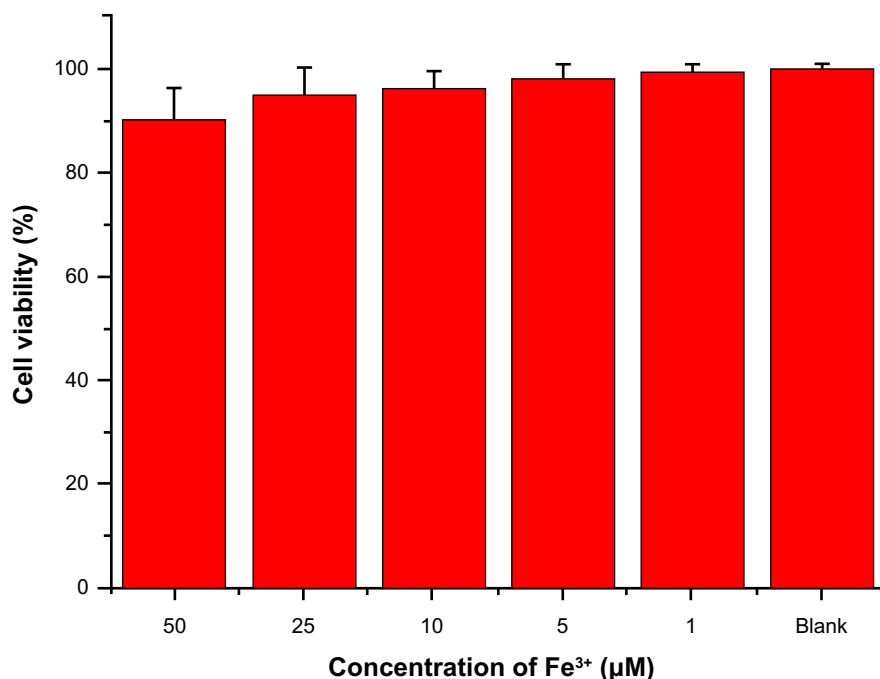
Figure 8 Viability of L02 cells incubated with bovine serum albumin surface functionalized hydrophobic superparamagnetic iron oxide nanoparticles for 24 hours was measured using the 3-(4, 5-dimethylthiazol-2-yl)-2, 5-diphenyl-tetrazolium bromide assay.
Note: Viability measurements were normalized to cells grown in the absence of any nanoparticles.

attributable to the validity of the antibody-mediated targeting. The combination of optical and MR imaging is clinically advantageous, as shown in this study, as MRI provides anatomical investigation in vivo while high sensitivity is ensured by optical imaging.

This study reports a novel nanoparticle surface engineering approach. Upon conjugation with antibodies, the prepared nanoprobe has good cell targeted imaging capability. Also, their biodistribution, an in vivo imaging study, and an in vivo toxicity study will be considered in the next research plan in our laboratory.

Cytotoxicity study

In vitro cytotoxicity of BSA·SPIONs was evaluated against the normal L02 cell line using the MTT assay (Figure 8). After 24 hours incubation with BSA·SPIONs at various Fe^{3+} concentrations, the viability of L02 cells is over 80%, even at 50 µM of Fe^{3+}. It indicates hypotoxicity of BSA·SPIONs against normal L02 cells, which has great potential for in vivo imaging.

Conclusion

A novel and facile approach was developed for surface functionalization of SPIONs with BSA biomacromolecule. BSA·SPIONs have been found to exhibit excellent biocompatibility, colloidal stability, and high relaxivity. Nonspecific cellular binding has been effectively reduced by this new approach. Excellent performance of ^{dye}BSA·SPIONs-mAb bioconjugates are demonstrated in the bimodal imaging of pancreatic cancer cells. Several major advantages of the ^{dye}BSA·SPIONs-mAb bioconjugates, including simple synthesis, good biocompatibility and stability, high relaxivity, and targeted imaging, make these nanosystems ideal candidates as imaging CA and will show promise in early cancer diagnosis.

Acknowledgment

Supporting information available

Fourier transform infrared spectra, digital images of superparamagnetic iron oxide nanoparticles, fluorescent spectra of free Cy5 dye and ^{dye}bovine serum albumin surface functionalized hydrophobic superparamagnetic iron oxide nanoparticles, and confocal images are available free of charge via the Internet.

Disclosure

The authors report no conflicts of interest in this work.

References

1. Schneider G, Siveke JT, Eckel F, Schmid RM. Pancreatic cancer: basic and clinical aspects. *Gastroenterology*. 2005;128(6):1606–1625.
2. Jemal A, Siegel R, Ward E, Hao Y, Xu J, Thun MJ. Cancer statistics, 2009. *CA Cancer J Clin*. 2009;59(4):225–249.
3. Foy SP, Manthe RL, Foy ST, Dimitrijevic S, Krishnamurthy N, Labhasetwar V. Optical imaging and magnetic field targeting of magnetic nanoparticles in tumors. *ACS Nano*. 2010;4(9):5217–5224.
4. Wang QB, Han Y, Jiang TT, et al. MR Imaging of activated hepatic stellate cells in liver injured by CCl4 of rats with integrin-targeted ultrasmall superparamagnetic iron oxide. *Eur Radiol*. 2011;21(5):1016–1025.
5. Liu F, Laurent S, Fattahi H, Vander Elst L, Muller RN. Superparamagnetic nanosystems based on iron oxide nanoparticles for biomedical imaging. *Nanomedicine (Lond)*. 2011;6(3):519–528.
6. Cheng FY, Su CH, Yang YS, et al. Characterization of aqueous dispersions of Fe3O4 nanoparticles and their biomedical applications. *Biomaterials*. 2005;26(7):729–738.
7. Thorek DL, Chen AK, Czupryna J, Tsourkas A. Superparamagnetic iron oxide nanoparticle probes for molecular imaging. *Ann Biomed Eng*. 2006;34(1):23–38.
8. Bulte JW, Kraitchman DL. Iron oxide MR contrast agents for molecular and cellular imaging. *NMR Biomed*. 2004;17(7):484–499.
9. Sun S, Zeng H, Robinson DB, et al. Monodisperse MFe2O4 (M = Fe, Co, Mn) nanoparticles. *J Am Chem Soc*. 2004;126(1):273–279.
10. Yu WW, Chang E, Falkner JC, et al. Forming biocompatible and nonaggregated nanocrystals in water using amphiphilic polymers. *J Am Chem Soc*. 2007;129(10):2871–2879.
11. Xu C, Xu K, Gu H, et al. Dopamine as a robust anchor to immobilize functional molecules on the iron oxide shell of magnetic nanoparticles. *J Am Chem Soc*. 2004;126(32):9938–9939.
12. Niu D, Li Y, Qiao X, et al. A facile approach to fabricate functionalized superparamagnetic copolymer-silica nanocomposite spheres. *Chem Commun (Camb)*. 2008;(37):4463–4465.
13. Chen H, Wang L, Yeh J, et al. Reducing non-specific binding and uptake of nanoparticles and improving cell targeting with an antifouling PEO-b-PgammaMPS copolymer coating. *Biomaterials*. 2010;31(20):5397–5407.
14. Salvador-Morales C, Zhang L, Langer R, Farokhzad OC. Immunocompatibility properties of lipid-polymer hybrid nanoparticles with heterogeneous surface functional groups. *Biomaterials*. 2009;30(12):2231–2240.
15. Cho EC, Xie J, Wurm PA, Xia Y. Understanding the role of surface charges in cellular adsorption versus internalization by selectively removing gold nanoparticles on the cell surface with a I2/KI etchant. *Nano Lett*. 2009;9(3):1080–1084.
16. Kairdolf BA, Mancini MC, Smith AM, Nie S. Minimizing nonspecific cellular binding of quantum dots with hydroxyl-derivatized surface coatings. *Anal Chem*. 2008;80(8):3029–3034.
17. Bentzen EL, Tomlinson ID, Mason J, et al. Surface modification to reduce nonspecific binding of quantum dots in live cell assays. *Bioconjug Chem*. 2005;16(6):1488–1494.
18. Simpson CA, Agrawal AC, Balinski A, Harkness KM, Cliffel DE. Short-chain PEG mixed monolayer protected gold clusters increase clearance and red blood cell counts. *ACS Nano*. 2011;5(5):3577–3584.

19. Strable E, Bulte JWM, Moskowitz B, Vivekanandan K, Allen M, Douglas T. Synthesis and characterization of soluble iron oxide-dendrimer composites. *Chem Mater*. 2001;13(6):2201–2209.

20. Wakayama J, Sekiguchi H, Akanuma S, Ohtani T, Sugiyama S. Methods for reducing nonspecific interaction in antibody-antigen assay via atomic force microscopy. *Anal Biochem*. 2008;380(1):51–58.

21. Zhang B, Wang X, Liu F, Cheng Y, Shi D. Effective reduction of non-specific binding by surface engineering of quantum dots with bovine serum albumin for cell-targeted imaging. *Langmuir*. 2012;28(48): 16605–16613.

22. Zhang B, Li Q, Yin P, et al. Ultrasound-triggered BSA/SPION hybrid nanoclusters for liver-specific magnetic resonance imaging. *ACS Appli Mater Interfaces*. 2012;4(12):6479–6486.

23. Remsen LG, McCormick CI, Roman-Goldstein S, et al. MR of carcinoma-specific monoclonal antibody conjugated to monocrystal-line iron oxide nanoparticles: the potential for noninvasive diagnosis. *AJNR Am J Neuroradiol*. 1996;17(3):411–418.

24. Huang J, Wang L, Lin R, et al. Casein-coated iron oxide nanoparticles for high MRI contrast enhancement and efficient cell targeting. *ACS Appl Mater Interfaces*. 2013;5(11):4632–4639.

25. Huang J, Xie J, Chen K, et al. HSA coated MnO nanoparticles with prominent MRI contrast for tumor imaging. *Chem Commun (Camb)*. 2010;46(36):6684–6686.

26. Lee JH, Lee K, Moon SH, Lee Y, Park TG, Cheon J. All-in-one target-cell-specific magnetic nanoparticles for simultaneous molecular imaging and siRNA delivery. *Angew Chem Int Ed Engl*. 2009;48(23): 4174–4179.

27. Bausch D, Thomas S, Mino-Kenudson M, et al. Plectin-1 as a novel biomarker for pancreatic cancer. *Clin Cancer Res*. 2011;17(2):302–309.

28. Kelly KA, Bardeesy N, Anbazhagan R, et al. Targeted nanoparticles for imaging incipient pancreatic ductal adenocarcinoma. *PLoS Med*. 2008;5(4):e85.

29. Dong A, Ye X, Chen J, et al. A generalized ligand-exchange strategy enabling sequential surface functionalization of colloidal nanocrystals. *J Am Chem Soc*. 2011;133(4):998–1006.

30. Yang Q, Gong X, Song T, et al. Quantum dot-based immunochromatog-raphy test strip for rapid, quantitative and sensitive detection of alpha fetoprotein. *Biosens Bioelectron*. 2011;30(1):145–150.

31. Mahmoudi M, Simchi A, Imani M, et al. A new approach for the in vitro identification of the cytotoxicity of superparamagnetic iron oxide nanoparticles. *Colloids Surf B Biointerfaces*. 2010;75(1):300–309.

32. Carter DC, Ho JX. Structure of serum albumin. *Adv Prot Chem*. 1994;45:153–203.

33. Huang X, Li BY, Zhang H, Hussain I, Liang LY, Tan BE. Facile preparation of size-controlled gold nanoparticles using versatile and end-functionalized thioether polymer ligands. *Nanoscale*. 2011;3(4): 1600–1607.

34. Cui Y, Gong XQ, Zhu SJ, et al. An effective modified method to prepare highly luminescent, highly stable water-soluble quantum dots and its preliminary application in immunoassay. *J Mater Chem*. 2012;22(2): 462–469.

35. Tang ZH, Xu B, Wu BH, Germann MW, Wang GL. Synthesis and structural determination of multidentate 2,3-dithiol-stabilized Au clusters. *J Am Chem Soc*. 2010;132(10):3367–3374.

36. Lutz HD, Himmrich J, Schmidt M. Lattice vibration spectra. Part LXXXVI. Infrared and Raman spectra of baryte-type TlClO4, TlBF4, and NH4BF4 single crystals and of 11B-enriched NH4BF4. *J Alloys Compd*. 1996;241(1–2):1–9.

37. Wright AK, Thompson MR. Hydrodynamic structure of bovine serum albumin determined by transient electric birefringence. *Biophys J*. 1975;15(2 Pt 1):137–141.

38. Burtea C, Laurent S, Murariu O, et al. Molecular imaging of alpha v beta3 integrin expression in atherosclerotic plaques with a mimetic of RGD peptide grafted to Gd-DTPA. *Cardiovasc Res*. 2008;78(1):148–157.

39. Monopoli MP, Walczyk D, Campbell A, et al. Physical-chemical aspects of protein corona: relevance to in vitro and in vivo biological impacts of nanoparticles. *J Am Chem Soc*. 2011;133(8):2525–2534.

40. Amiri H, Bordonali L, Lascialfari A, et al. Protein corona affects the relaxivity and MRI contrast efficiency of magnetic nanoparticles. *Nanoscale*. 2013;5(18):8656–8665.

41. Sakai G, Nakata S, Uda T, Miura N, Yamazoe N. Highly selective and sensitive SPR immunosensor for detection of methamphetamine. *Electrochim Acta*. 1999;44(21–22):3849–3854.

42. Festag G, Steinbruck A, Wolff A, Csaki A, Moller R, Fritzsche W. Optimization of gold nanoparticle-based DNA detection for microarrays. *J Fluoresc*. 2005;15(2):161–170.

43. Mirshafiee V, Mahmoudi M, Lou KY, Cheng JJ, Kraft ML. Protein corona significantly reduces active targeting yield. *Chem Commun (Camb)*. 2013;49(25):2557–2559.

44. Salvati A, Pitek AS, Monopoli MP, et al. Transferrin-functionalized nanoparticles lose their targeting capabilities when a biomolecule corona adsorbs on the surface. *Nat Nanotechnol*. 2013;8(2):137–143.

Supplementary materials
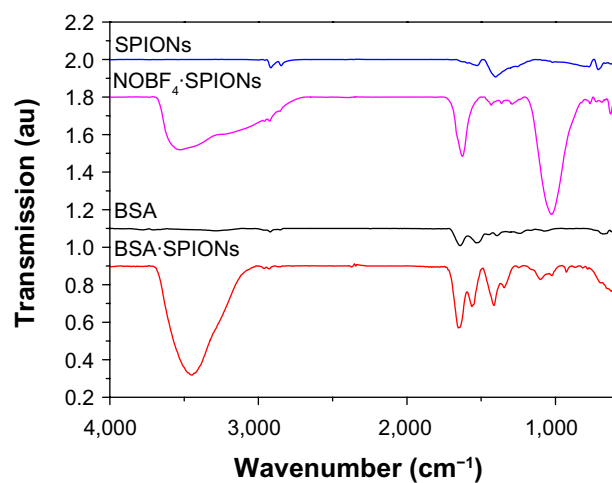
Figure S1 Fourier transform infrared spectra of the original superparamagnetic iron oxide nanoparticles, tetrafluoroborate superparamagnetic iron oxide nanoparticles, bovine serum albumin, and bovine serum albumin surface functionalized hydrophobic superparamagnetic iron oxide nanoparticles.

Abbreviations: BSA, bovine serum albumin; BSA·SPIONs, bovine serum albumin surface functionalized hydrophobic superparamagnetic iron oxide nanoparticles; NOBF$_4$·SPIONS; tetrafluoroborate superparamagnetic iron oxide nanoparticles; SPIONS, superparamagnetic iron oxide nanoparticles.
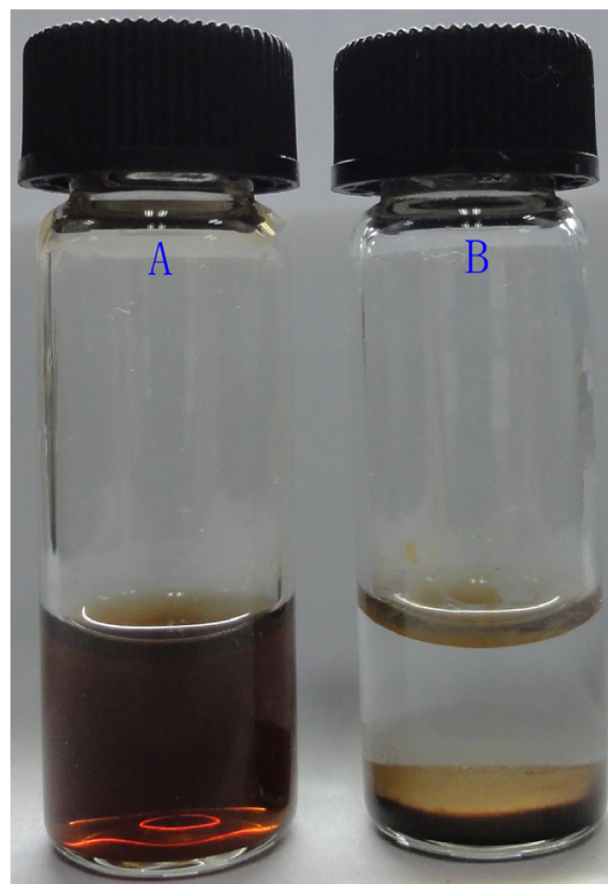
Figure S2 Optical photographs of bovine serum albumin surface functionalized hydrophobic superparamagnetic iron oxide nanoparticles showing the necessity of dialysis to remove the dimethylformamide.

Notes: The dispersion of dialyzed bovine serum albumin surface functionalized hydrophobic superparamagnetic iron oxide nanoparticles is optically clear (**A**) while the sample without dialysis has obvious sediments (**B**).
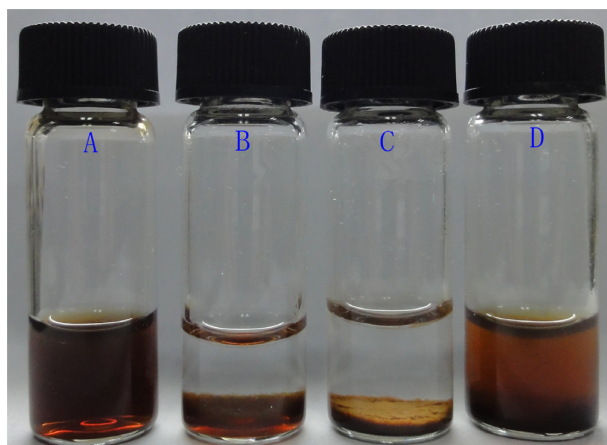
**Figure S3** Digital images of superparamagnetic iron oxide nanoparticles.
Notes: Superparamagnetic iron oxide nanoparticles redispersed in deionized water and functionalized by various water soluble polymers including (**A**) bovine serum albumin, (**B**) dopamine hydrochloride, (**C**) NH2-polyethylene glycol-COOH (molecular weight of 2 kDa), and (**D**) NH2-polyethylene glycol-SH (molecular weight of 3.5 kDa) after 7 days of storage at room temperature.
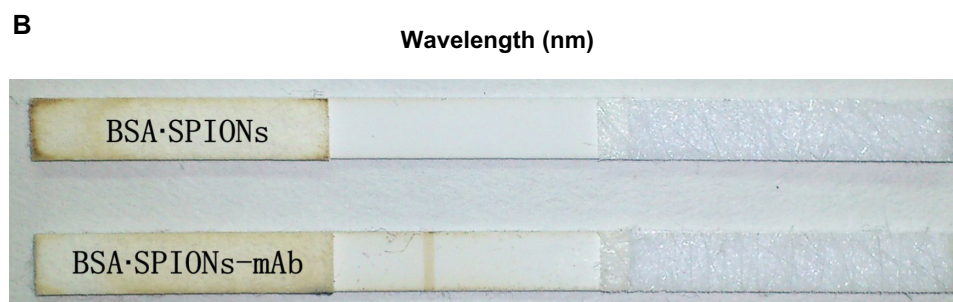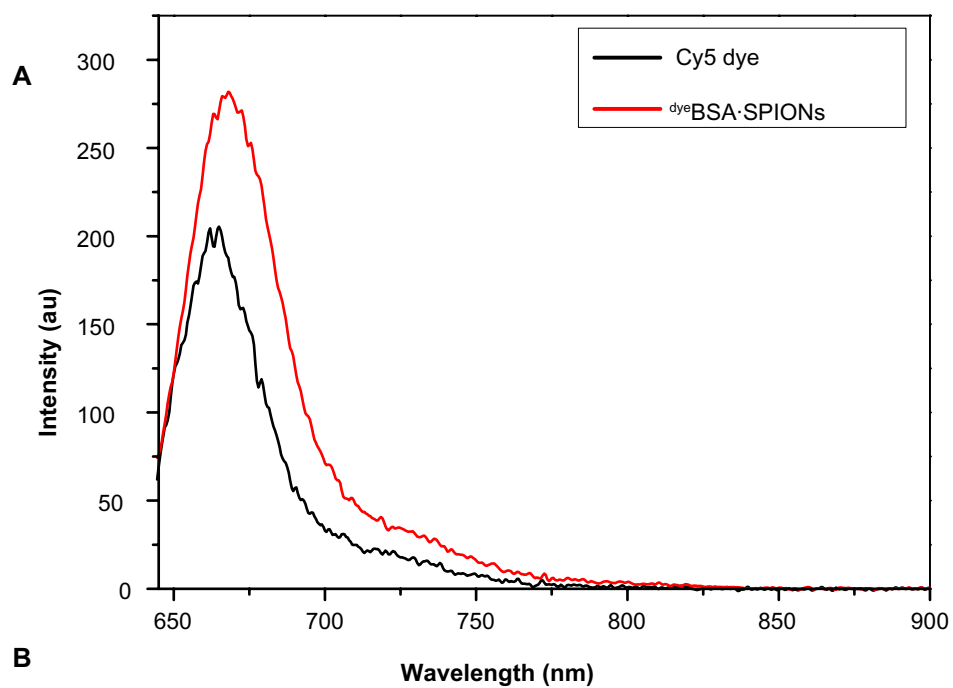
Figure S4 Fluorescence spectra and test strips of functionalized hydrophobic superparamagnetic iron oxide nanoparticles.
Notes: (**A**) Fluorescence spectra of free Cy5 dye and ^{dye}bovine serum albumin surface functionalized hydrophobic superparamagnetic iron oxide nanoparticles (^{dye}BSA·SPIONs). (**B**) Digital images of test trips using ^{dye}BSA·SPIONs and ^{dye}BSA·SPIONs-monoclonal antibody bioconjugates.
Abbreviations: ^{dye}BSA·SPIONs, ^{dye}bovine serum albumin surface functionalized hydrophobic superparamagnetic iron oxide nanoparticles; ^{dye}BSA·SPIONs-mAb, ^{dye}BSA·SPIONs-monoclonal antibody bioconjugates.
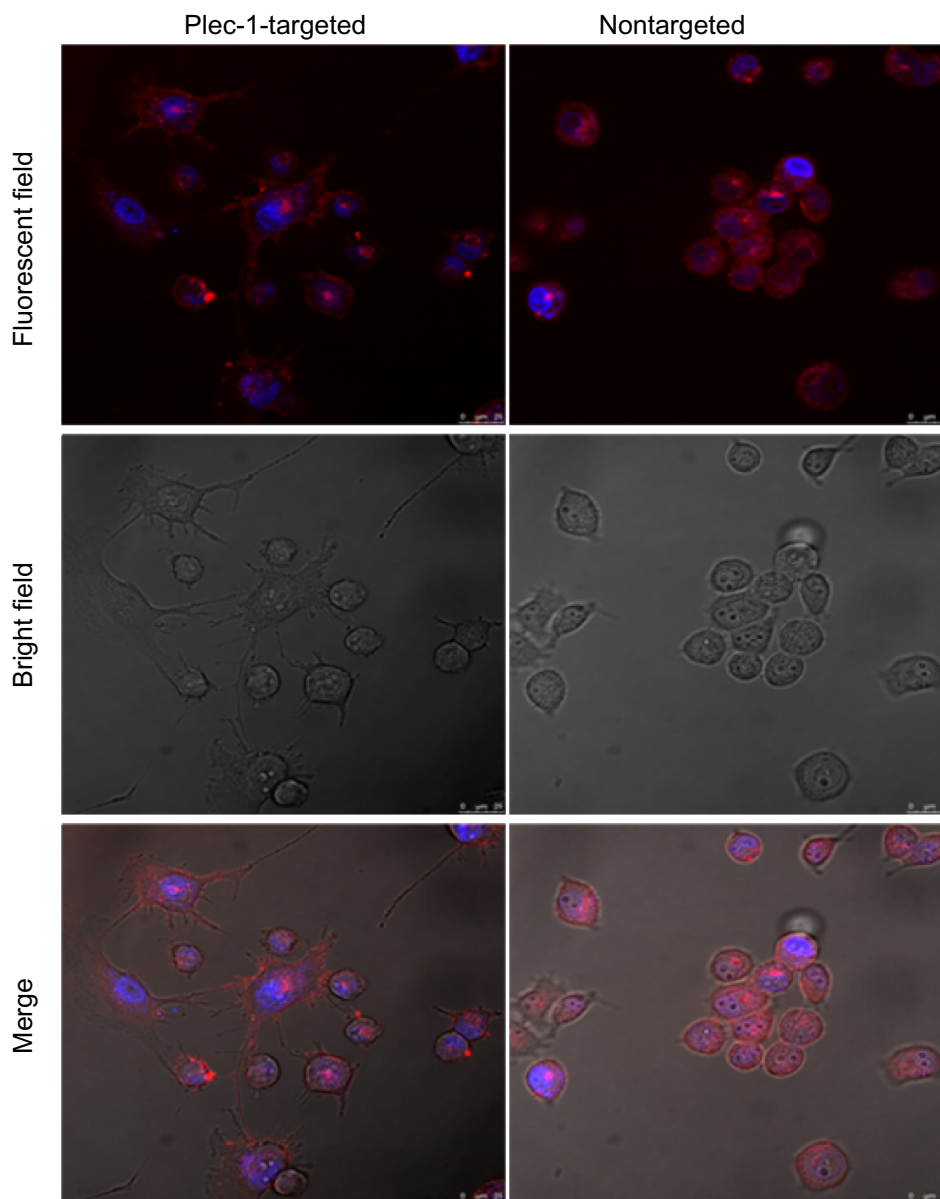
Figure S5 Panc-1 cells (Plec-1-positive) were incubated with Plec-1-targeted and nontargeted ^dyebovine serum albumin surface functionalized hydrophobic superparamagnetic iron oxide nanoparticles for 30 minutes.

Notes: As the incubation time increases, cellular internalization of nanoparticles (in red) results in nonspecific signals for nontargeted ^dyebovine serum albumin surface functionalized hydrophobic superparamagnetic iron oxide nanoparticles conjugates. Nuclei were labeled by 4′,6-diamidino-2-phenylindole in blue.